

A novel inorganic–organic hybrid compound constructed from copper(II)-monosubstituted polyoxometalates and poly(amidoamine)

Shen Lin · Xiaofeng Zhang · Minghong Luo

Received: 11 July 2008 / Revised: 5 November 2008 / Accepted: 6 November 2008 / Published online: 27 November 2008
© Springer-Verlag 2008

Abstract A novel inorganic–organic hybrid compound constructed from copper(II)-monosubstituted polyoxometalate $\text{Na}_5\text{PW}_{11}\text{Cu}(\text{H}_2\text{O})\text{O}_{39}$ (PW_{11}Cu) and poly(amidoamine) (PAMAM) dendrimer was prepared at room temperature in an aqueous solution. The title compound $\text{PW}_{11}\text{Cu}/\text{PAMAM}$ was characterized by Fourier transform infrared spectroscopy, X-ray photoelectron spectroscopy, and X-ray diffraction, indicating that the PW_{11}Cu was chemically anchored to PAMAM. The compound was first used as a bulk-modifier to fabricate a chemically modified carbon paste electrode (CPE) by direct mixing. The $\text{PW}_{11}\text{Cu}/\text{PAMAM}$ bulk-modified CPE showed well-defined cyclic voltammograms with four redox couples in 0.2 M NaAc buffer solution and high electrocatalytic activity for the reduction of hydrogen peroxide and nitrite. Furthermore, the CPE revealed good stability due to the insolubility of the title compound and the interaction between PW_{11}Cu and PAMAM.

Keywords Inorganic–organic · Hybrid · Polyoxometalates · Poly(amidoamine) · Electrocatalytic reduction

Introduction

Polyoxometalates (POMs) have won particular attention for their applications in the fields such as medicine, biology, catalysis, and materials due to their chemical, structural, and electronic versatility [1]. One of the most important

properties of these metal oxide clusters is the capability for reversible multivalence reduction, forming mixed-valence species [2–5], which makes them very useful in the field of electrocatalysis. The transition-metal-substituted polyoxometalates (TMSPs) have attracted much interest because of their catalytic reactivity similar to metalloporphyrin [6]. Various TMSPs have been prepared and their electrochemical and electrocatalysis were studied. Among the electrochemical investigation of TMSPs, the copper(II) substituted polyoxometalates are very popular [3, 7–10]. However, most of these studies focused mainly on the electrochemistry behavior in homogeneous aqueous solution. Immobilizing TMSPs onto electrode surfaces while maintaining and enhancing their beneficial properties, is fascinating to chemists.

Dendrimers are known for a number of potential applications in supramolecular chemistry, nanosciences, biology, and medicine, and many of their transition-metal complexes are especially promising in catalysis [11]. Poly (amidoamine) (PAMAM) with *hydroxyl* as terminal groups has been proven to be a useful template by providing reactive sites at its periphery [12]. A layer-by-layer (LBL) deposition technique based on electrostatic attraction of oppositely charged species has been used to fabricate multilayer films consisting of POMs and PAMAM dendrimer [13–16]. Recently, the POMs–PAMAM hybrid has been reported to be synthesized by covalent assembly and used as active and recoverable oxidation catalysts [17]. In this paper, the inorganic–organic hybrid compound containing copper (II)-monosubstituted polyoxometalates PW_{11}Cu and PAMAM dendrimer was synthesized in aqueous solution by covalent assembly and used to fabricate a three-dimensional bulk-modified CPE by direct mixing. In the present configuration, the graphite powder contributes to the conductivity; Nujol is as a pasting liquid; the inorganic component (PW_{11}Cu) provides the electrocatalysis for the

S. Lin (✉) · X. Zhang · M. Luo
College of Chemistry and material Sciences,
Fujian Normal University,
Fujian,
Fuzhou 350007, China
e-mail: shenlin@fjnu.edu.cn

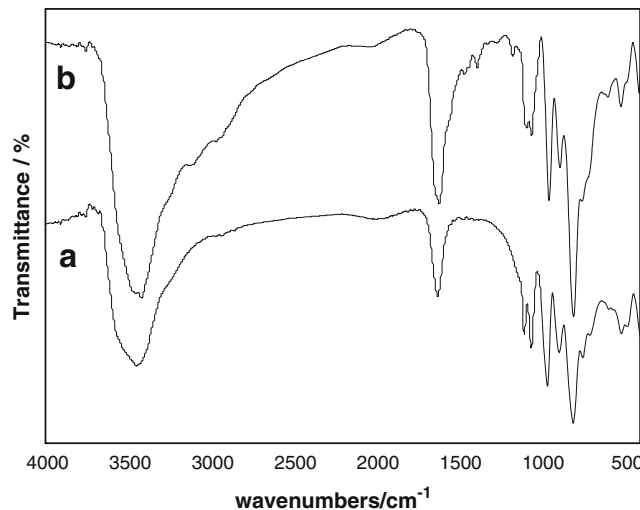


Fig. 1 IR spectra of **a** PW₁₁Cu and **b** PW₁₁Cu-PAMAM

reduction of hydrogen peroxide and nitrite; the organic component (PAMAM), on the one hand, makes the hybrid compound insoluble in analytic solution and avoids bleeding of the modifier; on the other hand, it displays such a high affinity toward the paste that stabilizes the bulk-modified CPE, which makes the CPE remarkably stable. To our knowledge, it is the first example of fabrication of bulk-modified CPE consisting of transition metal monosubstituted POMs and a soft organic dendrimer.

Experimental

All chemicals were of analytical grade and used without further purification. PAMAM dendrimers (Generation-1) were commercially provided and partially prepared following the method reported [18]. Na₅[Cu(H₂O)PW₁₁O₃₉] 3H₂O was synthesized according to the reference [19]. Fourier transform infrared spectroscopy (FTIR) (cm⁻¹): 1,101, 1,060, 961, 890, 805, 745, 700. DR-UV-Vis(nm): 260, 340, 870. The FTIR and UV-Vis spectra were in agreement with those

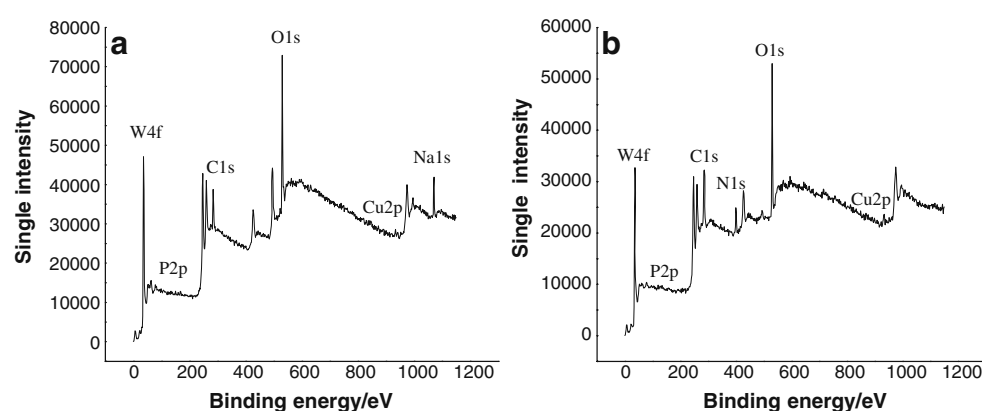
obtained from the literature [19]. Anal.Calcd(found): Na 3.95 (3.76), P 1.07(1.00), W 71.05(68.85), Cu 2.18(2.31).

The PW₁₁Cu-PAMAM composite was prepared as follows: In a 100-mL one-necked flask, 4.7 g (1.6 mmol) of PW₁₁Cu were dissolved in 10 mL of H₂O. Of PAMAM, 0.2 g was dispersed in 25 mL of H₂O at pH 6–7 and then was added dropwise into the flask with stirring at room temperature for 24 h, producing a blue precipitate. The product was filtered and washed with deionized water and ethanol several times and then dried in vacuum at 50 °C overnight. The yield was 80% (based on PAMAM). Anal. Calcd(found) for the composite: C 8.44(8.36), H 2.21(2.14), N 4.35(4.30), P 1.10(1.12), W 69.02(68.88), Cu 2.19(2.18).

FTIR spectra were obtained on a Nicolet AVATAR 360 FTIR spectrometer (KBr pellets, 4,000–400 cm⁻¹). X-ray photoelectron spectroscopy(XPS) was determined on Quantum-2000 Scanning ESCA Microprobe system using Al mono K radiation as the excitation source and with a pass energy of 46.95 eV. The binding energies were referenced to the C 1s level (284.6 eV) due to contaminant carbon as a reference. Powder X-ray diffraction (XRD) was performed on a Siemens D5005 X-ray diffractometer with Cu K α radiation. Elemental analyses were carried out using a Perkin Elmer Model 240C elemental analyzer.

The PW₁₁Cu-PAMAM-CPE was fabricated as follows: 1.0 g graphite powder and 60 mg PW₁₁Cu-PAMAM were mixed by a mortar and pestle to achieve a uniform and dry mixture. Nujol, 1.0 mL, was added to the mixture and blended uniformly, then the resulting paste was inserted in the bottom of a hollow graphite electrode (inner diameter 3 mm, outer diameter 5 mm, mixture depth 4.5 mm). The electrochemical experiments were carried out on a CHI 660 electrochemical workstation at room temperature(25–30°C) under nitrogen atmosphere. A platinum gauze was used as the auxiliary electrode. The PW₁₁Cu-PAMAM-CPE was used as the working electrode. The reference electrode was an Ag|AgCl| KCl_{sat} (Metrohm). Buffer solution was prepared from 0.2 M NaAc + HAc (pH=4.7).

Fig. 2 XPS spectra of **a** PW₁₁Cu and **b** PW₁₁Cu-PAMAM



Results and discussion

To probe the structure and formation of the title compound, FTIR, XPS, XRD experiments were conducted. The FTIR spectra are shown in Fig. 1. Three characteristic vibration bands of ν_{as} ($W=O_d$), ν_{as} ($W-O_b-W$), and ν_{as} ($W-O_c-W$) were observed at 951, 886, and 803 cm^{-1} , respectively, showing that the compound retained the Keggin structure type. The decreases in the intensities of the splitting of P–O bond and some shifts of W–O–W bonds might be attributed to interaction between PW_{11}Cu cluster and PAMAM. The N–H stretch bands (3,289, 3,092 cm^{-1}) of the hybrid composite overlapped the OH stretching vibration band of water molecule. The weak sawtooth shape peaks appearing at 1,548, 1,463, 1,386, 1,170 cm^{-1} showed the presence of the PAMAM molecules in the hybrid composite.

X-ray photoelectron spectroscopy (XPS) reveals the presence of PAMAM and PW_{11}Cu in the hybrid (Fig. 2). The N1s spectral region of PW_{11}Cu -PAMAM is shown in Fig. 3. A main peak with a binding energy of 399.8 eV is characteristic of covalently bonded nitrogen [20]. A small shoulder peak with a binding energy of ~401.5 eV may be assigned to the partial protonation of some free amine groups by exposure to water solution [21]. The Cu2p binding energy is observed at 933.3 eV for PW_{11}Cu and 931.9 eV for the hybrid compound. The decrease of value reflected the increased electron density on Cu atom in the hybrid on account of the coordination between Cu and N atoms [22].

The characteristic XRD peaks for the compound PW_{11}Cu were observed in 10–60° as shown in Fig. 4 a, but broadened peaks were appeared in Fig. 4 b for PW_{11}Cu /PAMAM. This may result from the dispersion of PAMAM.

The cyclic voltammetry for PW_{11}Cu -PAMAM-CPE in pH 4.7 buffer solution was performed (Fig. 5). Two sets of redox peaks were observed in the negative potential range of –0.6 to –1.0 V, which derive from the redox process of W–O

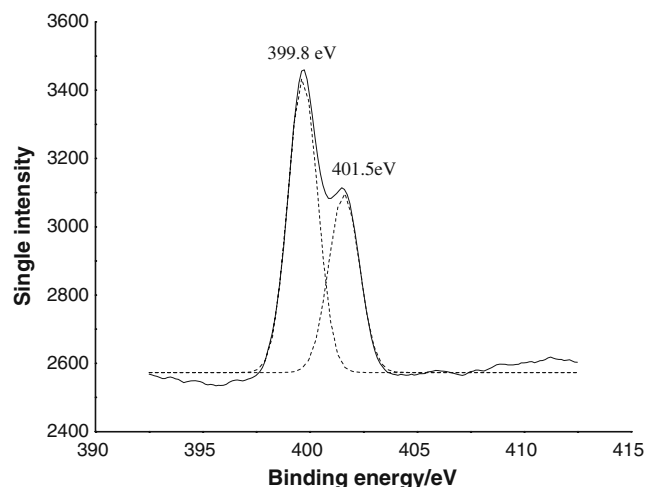


Fig. 3 XPS spectra for N1s region of PW_{11}Cu -PAMAM

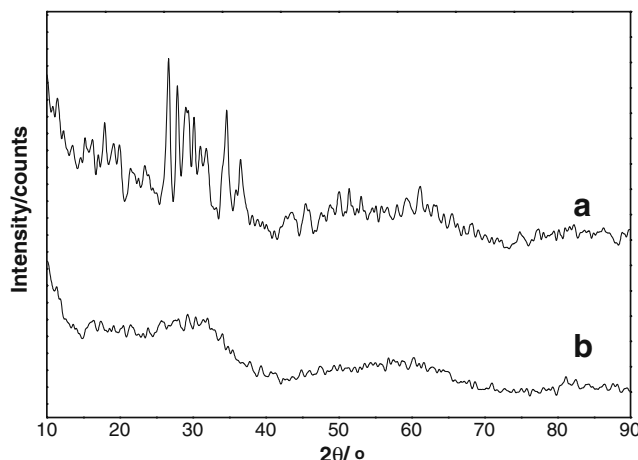


Fig. 4 XRD patterns of **a** PW_{11}Cu and **b** PW_{11}Cu -PAMAM

framework. It is worth noting that two overlapped reduction peaks(I,II) are observed at –0.14 and –0.28 V, respectively, which corresponds to the two one-electron reduction of Cu^{II} ions [7, 23]. It is different from one single two-electron Cu^{II} reduction peaks observed in homogeneous solution [3, 24]. Consistent with the result of X-ray photoelectron spectroscopy, the data of cyclic voltammetry also suggested that there are some substituted special interactions between the transition metal atoms of PW_{11}Cu and PAMAM.

The effect of scan rates on electrochemical behavior for the CPE was investigated in pH 4.7 buffer solution (Fig. 6). The plots of peak current versus scan rate was shown in Fig. 7. At scan rates lower than 0.10 Vs^{-1} , the cathodic peak current was proportional to scan rate, which indicates the redox process is surface-controlled. However, at scan rates higher than 0.10 Vs^{-1} , the $\log I$ was proportional to the

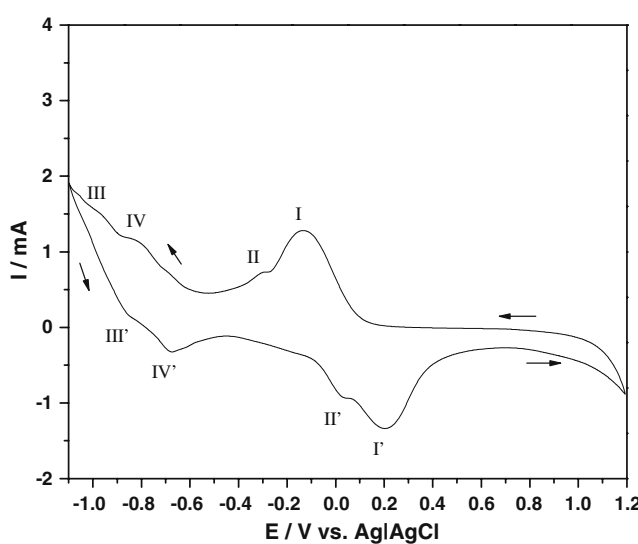


Fig. 5 CV of PW_{11}Cu -PAMAM-CPE in NaAc/HAc buffer solution, the scan rate were 0.04 Vs^{-1}

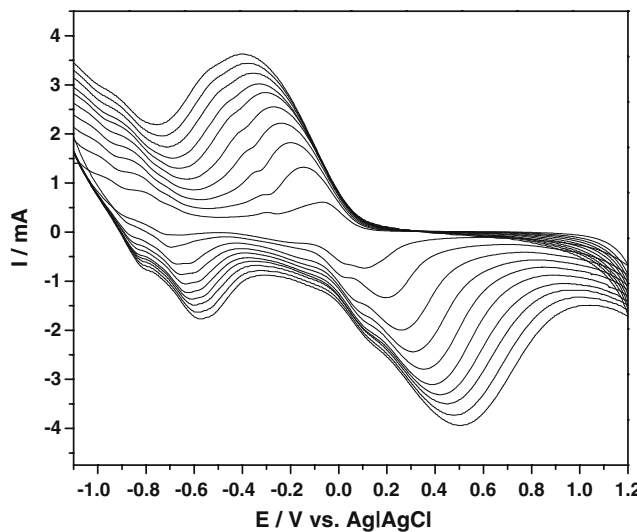


Fig. 6 CV of $\text{PW}_{11}\text{Cu}-\text{PAMAM}-\text{CPE}$ at different scan rates, from inner to outer: 0.02, 0.04, 0.06, 0.08, 0.10, 0.12, 0.14, 0.16, 0.18, and 0.20 Vs^{-1}

$\log V$ which indicates that the redox process is quasireversible surface electrode reaction.

The electrocatalytic activity of $\text{PW}_{11}\text{Cu}-\text{PAMAM}-\text{CPE}$ was evaluated by reduction of H_2O_2 or NaNO_2^- . The direct reduction of H_2O_2 or NaNO_2^- at a bare electrode requires a large overpotential and no obvious response is observed in the range of from +1.0 to -1.0 V. However, with the addition of H_2O_2 (Fig. 8), four reduction peak currents (I, II, III, IV) increase while the corresponding oxidation peak currents (I' , II' , III' , IV') decrease when using $\text{PW}_{11}\text{Cu}-\text{PAMAM}-\text{CPE}$, suggesting that Cu-reduced species and W-reduced species all possess electrocatalytic activity to H_2O_2 reduction. Inset shows the linear relationship between the Cu-centered catalytic currents (I) and H_2O_2 concentration.

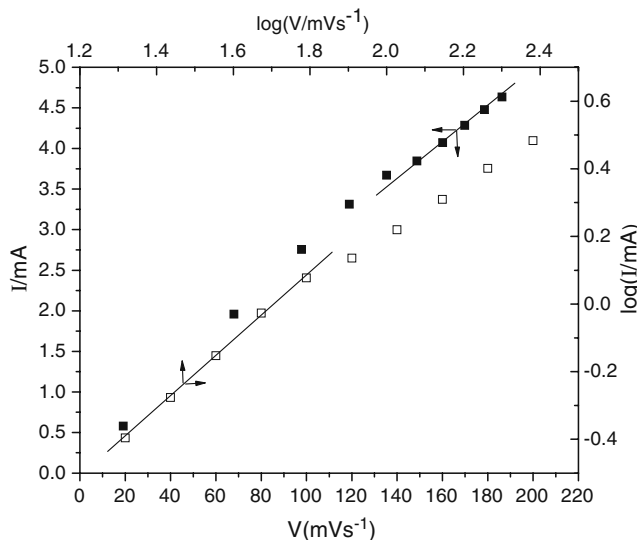


Fig. 7 Dependence of cathodic peak (I) current on scan rates

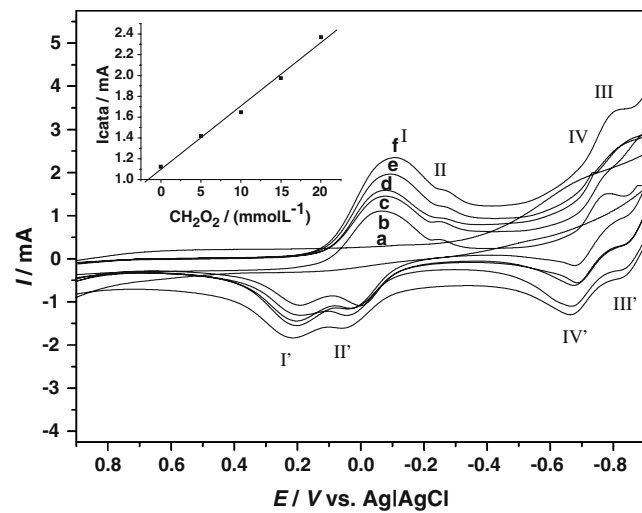


Fig. 8 **a** CV of a bare CPE in the $20 \text{ mM} \text{H}_2\text{O}_2 + 0.2 \text{ M} (\text{NaAc} + \text{HAc})$ solution and CV of $\text{PW}_{11}\text{Cu}-\text{PAMAM}-\text{CPE}$ in $0.2 \text{ M} (\text{NaAc} + \text{HAc})$ at different H_2O_2 concentrations (mM): **b** 0, **c** 5, **d** 10, **e** 15, **f** 20, the scan rate were 0.04 Vs^{-1} . Inset: dependence of the catalytic current on concentrations of H_2O_2

It was also found that the $\text{PW}_{11}\text{Cu}-\text{PAMAM}-\text{CPE}$ exhibited catalytic activity toward the reduction of NO_2^- (Fig. 9). The electrocatalysis occurs at the third (III–III') and the fourth (IV–IV') peaks of the CPE; with the addition of NO_2^- , the cathodic currents of the waves are enhanced, and the corresponding oxidation peaks decreased, while peaks I and II are almost unaffected by the addition of NO_2^- . The result indicates that NaNO_2 is only reduced by W-reduced species. Inset shows the linear relationship between the catalytic currents (III) and NO_2^- concentration.

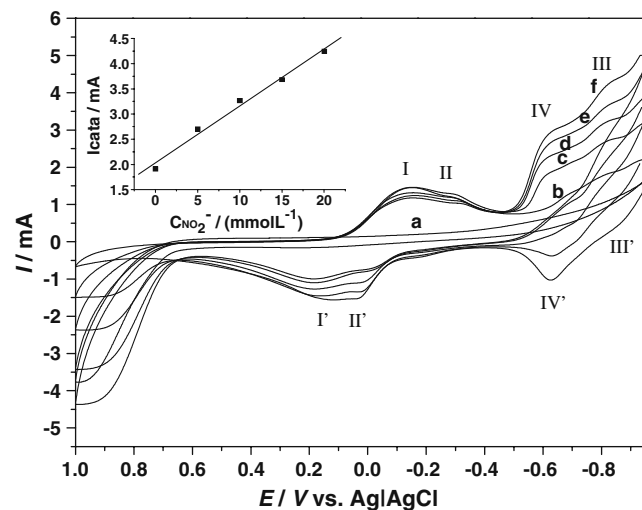


Fig. 9 **a** CV of a bare CPE in the $20 \text{ mM} \text{NO}_2^- + 0.2 \text{ M} (\text{NaAc} + \text{HAc})$ solution and CV of $\text{PW}_{11}\text{Cu}-\text{PAMAM}-\text{CPE}$ in $0.2 \text{ M} (\text{NaAc} + \text{HAc})$ at different NO_2^- concentrations (mM): **b** 0, **c** 5, **d** 10, **e** 15, **f** 20, the scan rate were 0.04 Vs^{-1} . Inset: dependence of the catalytic current on concentrations of NO_2^-

Compared with POMs-modified film electrodes fabricated with conventional methods, the three-dimensional PW_{11}Cu –PAMAM–CPE can be renewed easily and a fresh surface exposed by squeezing a little carbon paste whenever needed. When the potential range was maintained at -1.0 to $+1.0$ V, the peak currents only decreased 5% over 500 cycles at a rate of 0.04 Vs^{-1} , which indicated that PW_{11}Cu –PAMAM–CPE are stable. The peak currents almost keep unchanged after stored at room temperature for 2 months. The remarkable stability of PW_{11}Cu –PAMAM–CPE can be ascribed primarily to the insolubility of the hybrid compound and high charges of PW_{11}Cu entrapped in PAMAM.

Conclusion

The hybrid compound composed of PAMAM dendrimer and Cu monosubstituted polyoxometalate can be synthesized in an aqueous solution. The primary Keggin structure of TMSP remained intact after incorporating it into PAMAM, and the covalent interactions existed between PW_{11}Cu and PAMAM. The composite was firstly used as a bulk-modifier to fabricate a chemically modified carbon paste electrode and exhibited good electrocatalytic activity for the reduction of hydrogen peroxide and nitrite.

Acknowledgements This work was supported by the National Natural Science Foundation of China (No. 20771024) and Natural Science Foundation of Fujian Province of China (No. 2008J0142).

References

1. Sadakane M, Stekhan E (1998) Chem Rev 98:219b
2. Gamelas JAF, Gaspar AR, Evtuguin DV, Neto CP (2005) Appl Catal A: Gen 295:134
3. Keita B, Abdeljalil E, Nadjo L, Avisse B, Contant R, Canny J, Richet M (2000) Electrochim Commun 2:145
4. Chen S, Fa Y (2004) J Electroanal Chem 567:9
5. Wang L, Jiang M, Wang E, Lian S, Xu L, Li Z (2004) Mater Lett 58:683
6. Rong C, Anson FC (1994) Inorg Chem 33:1064
7. Liu J, Cheng L, Dong S (2002) Electroanal 14:569
8. Keita B, Nadjo L (2007) J Mol Catal A: Chem 262:190
9. Keita B, Abdeljalil E, Nadjo L, Contant R, Belgiche R (2006) Langmuir 22:10416
10. Keita B, Abdeljalil E, Nadjo L, Contant R, Belgiche R (2001) Electrochim Commun 3:56
11. Plault L, Hauseler A, Nlate S, Astruc D, Ruiz J, Gatard S, Neumann R (2004) Angew Chem Int Ed 43:2924
12. Bao C, Jin M, Lu R, Zhang T, Zhao Y (2003) Mater Chem Phys 81:160
13. Cheng L, Cox JA (2001) Electrochim Commun 3:285
14. Cheng L, Pace GE, Cox JA (2001) Electrochim Acta 46:4223
15. Kijak AM, Perdue RK, Cox JA (2004) J Solid State Electr 8:376
16. Sun L, Ca DV, Cox JA (2005) J Solid State Electr 9:816
17. Zhang X, Lin S, Luo G (2007) Chinese J Chem 25:323
18. Bosman AM, Janssen HM, Meijer EW (1999) Chem Rev 99:1665
19. He H, Sun T, Jiang D (1994) Chinese J Inorg Chem 10:272
20. Rar A, Curry M, Barnard JA, Street SC (2002) Tribol Lett 12:87
21. Rahman KMA, During CJ, Turro NJ, Tomalia DA (2000) Langmuir 16:10154
22. Xu L, Li M, Wang E (2002) Mater Lett 54:303
23. Pichon C, Mialane P, Dolbecq A, Marrot J, Riviere E, Keita B, Nadjo L, Sechersse F (2007) Inorg Chem 46:5292
24. Gamelas JAF, Balula MS, Carapuca HM, Cavaleiro AMV (2003) Electrochim Commun 5:378